

## STRUCTURE NOTE

## Crystal Structure of a Putative Phosphinothricin Acetyltransferase (PA4866) from *Pseudomonas aeruginosa* PAC1

Anna M. Davies, Renée Tata, Riaz Agha, Brian J. Sutton, and Paul R. Brown\*

Randall Division of Cell and Molecular Biophysics, King's College London, London, UK

**Introduction.** In the genome of *P. aeruginosa* PAO 1 (<http://www.pseudomonas.com/>) the gene PA4866 encodes a 172 amino acid protein (pita) belonging to the GCN5 family of acetyl transferases (PF00583). Blast searches reveal similar enzymes in a wide range of Gram-negative and Gram-positive organisms. These enzymes are listed either as hypothetical proteins or as putative phosphinothricin acetyl transferases (PAT). PAT is expressed in *Streptomyces hygroscopicus*<sup>1</sup> and *S. viridochromogenes*,<sup>2</sup> and catalyzes the acetylation of phosphinothricin, a glutamate analog widely used as a herbicide, which exerts its phytotoxic effect on plants<sup>3</sup> by inhibiting glutamine synthetase.<sup>4</sup> Pita displays 45 and 42% sequence similarity (37 and 35% sequence identity) with the two PAT enzymes, respectively. We now report the crystal structure of this enzyme, as a basis for investigating its function.

**Experimental Procedures.** *Purification of Se-met pita.* The pita gene (PA4866) was amplified by PCR from *Pseudomonas aeruginosa* PAC1 (8602) genomic DNA and cloned into the NdeI and BamHI sites of vector pET 24a (Novagen). PAC1 displays minor sequence differences compared with strain PAO1 in the *Pseudomonas* genome database. In gene PA4866, the only difference between the two strains is the nucleotide change (PAO1)A139G (PAC1), resulting in the amino acid change T47A. Recombinant plasmid DNA was used to transform met- *Escherichia coli* strain B834 (DE3) (Novagen). Cells were grown in 400 mL methionine-supplemented M9 medium to an OD<sub>600</sub> = 1, resuspended in fresh medium without methionine, and grown at 37°C for 6 h before adding 50 mg Se-met followed, after 30 min, by 1 mM IPTG. After 9.5 h growth at 37°C, cells were harvested by centrifugation, resuspended in 20 mL cold 50 mM Tris buffer, pH 7.2, 1 mM EDTA, 1 mM DTT, pH 7.2 (TED). After sonication, addition of 0.2 g streptomycin sulphate and centrifugation, 45% (w/v) ammonium sulphate was added to the supernatant. The precipitate was dissolved and dialysed against cold TED before loading on a Q-Sepharose (2 × 15 cm) column. Protein was eluted with a 400 mL linear gradient of 0–0.3 M NaCl in TED buffer, and the peak of 280 nm absorbing material eluting at 0.15 M NaCl was bulked and precipitated with 70% (w/v) ammonium sulphate. The precipitate

was dissolved in TED (2 mL), loaded on a Sephacryl 200 column (26 × 600 mm), and eluted with TED containing 0.15 M NaCl. Peak fractions (280 nm) were bulked, and the protein precipitated with ammonium sulphate (70% (w/v)) then dissolved in 0.25 mL TED and dialysed against TED. **Crystallization.** Crystals of Se-met pita were grown using the hanging drop vapor diffusion method. The reservoir solution contained 1 mL of 0.1 M HEPES at pH 7.3, 23–27% (w/v) PEG 8000, and 0.1% (w/v) azide. The drops contained 1 μL protein solution at 10 mg/mL, to which an equal volume of reservoir solution was added. The drops were kept at 291 K (±0.5) and crystals up to 200 μm in length appeared after 6 h. Crystals were flash-cooled in liquid nitrogen using reservoir solution containing 22% (v/v) glycerol.

**Data collection and processing.** A SAD dataset was collected at Stn 14.2, Synchrotron Radiation Source, Daresbury, UK (λ = 0.975 Å, d = 160 mm) and processed with DENZO<sup>5</sup> and the CCP4 suite of programs.<sup>6</sup> The crystals belong to space group P4<sub>3</sub>2<sub>1</sub>2 with one molecule in the asymmetric unit.

**Structure determination.** The positions of three (out of a possible four) Se atoms were determined with SOLVE.<sup>7,8</sup> Refinement of the Se atom positions was performed using MLPHARE,<sup>9</sup> followed by density modification with DM.<sup>10,11</sup>

**Model building and refinement.** Manual model building was performed with QUANTA,<sup>12</sup> independently of other homologous structures available. Protein residues were modeled manually before solvent molecules and ligands were incorporated into the structure. Refinement was performed with CNS.<sup>13</sup> Five percent of reflections were used to calculate the R<sub>free</sub> value, used throughout the refinement process, with the exception of two final rounds for which all reflections were used. Ligand topology and parameter files were obtained from the HIC-Up data-

\*Correspondence to: Paul R. Brown, Randall Division of Cell and Molecular Biophysics, King's College London, 3rd Floor New Hunt's House, Guy's Campus, London Bridge, London SE1 1UL, UK. E-mail: paul.brown@kcl.ac.uk

Received 1 March 2005; Accepted 7 March 2005

Published online 13 September 2005 in Wiley InterScience (www.interscience.wiley.com). DOI: 10.1002/prot.20663



TABLE I. Data Processing and Refinement Statistics

Data processing		Refinement	
Unit cell dimensions (Å)	a = b = 79.930 c = 61.730	Resolution range (Å)	35.81–2.00
Resolution limit (Å)	2.00	No. of reflections	24,810
No. of unique reflections	13,388	No. of protein atoms	1334
Outer shell (Å)	2.05–2.00	No. of water molecules	213
Completeness (%) overall (outer shell)	96.1 (96.1)	Ave. B factor for protein atoms (Å <sup>2</sup> )	20.37
Multiplicity overall (outer shell)	12.8 (12.7)	Ave. B factor for water molecules (Å <sup>2</sup> )	36.12
I <sub>c</sub> : overall (outer shell)	4.6 (2.6)	R <sub>int</sub> (%) (all reflections)	19.74
R <sub>int</sub> (%) overall (outer shell)	10.0 (20.0)	R <sub>free</sub> (%) (5% of reflections)	22.94
		σ <sub>a</sub> coordinate error (Å)	0.10
		RMS deviation, bond lengths (Å)	0.018
		RMS deviation, bond angles (deg)	1.41

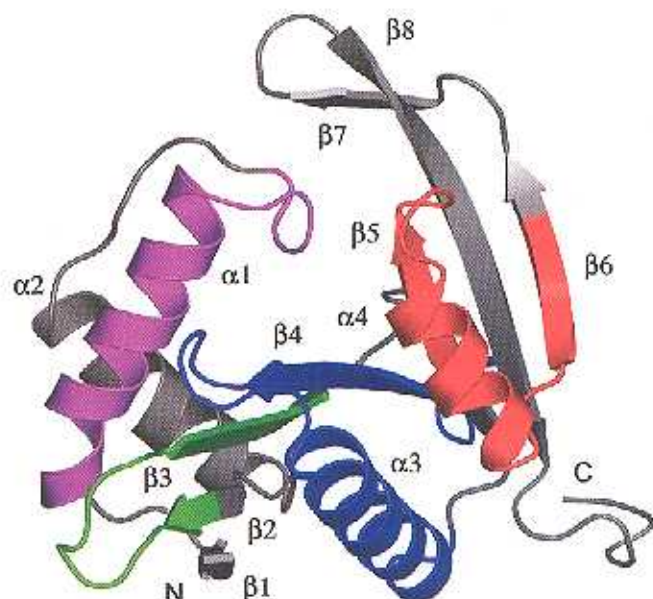


Fig. 1. Structure of the pita monomer. The GNAT motifs identified by Neuwald and Landeman<sup>17</sup> are identified by color, in order from the N- to the C-terminus, as follows: purple (motif C), green (motif D), blue (motif A), and red (motif B). Other regions of the polypeptide trace are colored gray.  $\alpha$ -Helices and  $\beta$ -strands are labeled  $\alpha$ 1–4 and  $\beta$ 1–8. The figure was drawn with Pymol.<sup>21</sup>

base.<sup>12</sup> The geometry of the final model was assessed with PROCHECK<sup>13</sup> and SFCHECK,<sup>14</sup> with 91.6% of residues adopting a favorable conformation and the remaining 8.4% in additional allowed regions. Data processing and refinement statistics are presented in Table I.

**Results and Discussion.** *Overall structure.* The refined structure of pita reveals a protein with an  $\alpha/\beta$  fold, comprising residues 3–172 (residues 1 and 2 were disordered). Its three-dimensional structure reveals an almost triangular arrangement of ordered secondary structural elements surrounding a central channel running through the protein, partially enclosed at one end by several loops (Fig. 1). Pita's overall fold can be described as two regions of antiparallel  $\beta$ -sheet, each flanked by  $\alpha$ -helices. The first antiparallel  $\beta$ -sheet (strands  $\beta$ 1–4) wraps around helix  $\alpha$ 3 on one side and is flanked on its opposite face by helix  $\alpha$ 1, which in turn, lies close to helix  $\alpha$ 2. The second antiparallel  $\beta$ -sheet comprises strands  $\beta$ 5–8, and is flanked by helix  $\alpha$ 4. This fold is remarkably similar to that recently re-

ported by Brunzelle et al. for the *Bacillus subtilis* YdaF protein, although in this structure strands  $\beta$ 6 and  $\beta$ 7, which are interrupted by a loop in pita, form a single strand.<sup>15</sup>

A search of the Pfam database<sup>16</sup> revealed that pita belongs to the GCN5-related N-Acetyltransferase (GNAT) superfamily (PF00583). Sequence analysis of the GNAT superfamily has led to the identification of four motifs (A–D) that are largely conserved among its members,<sup>17</sup> and subsequently, crystal structures allowed the secondary structure of these motifs to be determined.<sup>18,19</sup> Pita possesses all four conserved sequence motifs and their secondary structure is essentially identical to that already described for GNAT family members. These structural motifs are identified in Figure 1.

A search performed using the DALI server<sup>20</sup> revealed that structures have been solved for proteins displaying significant structural homology to pita. Structural comparisons were performed for 19 proteins with Z-scores ranging from 22.5 (PDB code 1VHS; 29% sequence identity; RMSD 1.7 Å) to 10.1 (1ON0; 14% sequence identity; RMSD 3.4 Å). The overall architecture of the acetyl-CoA fold ( $\alpha$ 1,  $\alpha$ 3,  $\alpha$ 4,  $\beta$ 2–6 in Fig. 1) was similar in all structures. An  $\alpha$ -helix equivalent to the  $\alpha$ 2 in pita was also frequently found. Apart from the flexible loops, the most structurally dissimilar regions were strands  $\beta$ 6–8, and the only structure with the same topology in this region was 1VHS, the highest scoring structure from the DALI server search.

Both 1VHS (from *Bacillus subtilis*) and pita have been assigned putative phosphinothricin acetyltransferase (PAT) activity on the basis of sequence similarities to known PATs. BLAST searches<sup>21</sup> revealed that these proteins are members of a large family for which little information is currently known. We now have two representative crystal structures for this family, which reveal a difference in the overall fold compared to other acetyltransferases, presumably reflecting a novel function. Studies are currently underway to determine the specificity and role of pita, which will shed further light on this new family of enzymes.

**Acknowledgments.** Atomic coordinates have been deposited in the Protein Data Bank<sup>22</sup> with the accession code 2BL1. We thank James Nicholson, Rob Kehoe, and Mike Macdonald for assistance during data collection at the



SRS. We thank the Wellcome Trust for a summer studentship for RA.

## REFERENCES

1. Thompson CJ, Mavea NR, Tizard R, Grameri R, Davies JF, Lauwereys M, Botterman J. Characterization of the herbicide-resistant gene bar from *Streptomyces hygroscopicus*. *EMBO J* 1987;6:2519–2523.
2. Strauch E, Wohlleben W, Publer A. Cloning of a phosphinothricin N-acetyltransferase gene from *Streptomyces viridochromogenes* Tu494 and its expression in *Streptomyces lividans* and *Escherichia coli*. *Gene* 1988;63:85–94.
3. Hoogland RF. Biochemical interactions of the microbial phyto-toxin phosphinothricin and analogs with plants and microbes. In: Cutler HG, Cutler SJ, editors. *Biologically active natural products: agrochemicals*. Boca Raton, FL: CRC Press; 1999. p 107.
4. Gill HS, Pfluegl GMU, Eisenberg D. The crystal structure of phosphinothricin in the active site of glutamine synthetase illuminates the mechanism of enzymatic action. *Biochemistry* 2001;40:1903–1912.
5. Otwinowski Z, Minor W. Processing of X-ray diffraction data collected in oscillation mode. *Methods Enzymol* 1997;276:307–326.
6. Collaborative Computational Project, Number 4. The CCP4 suite: programs for protein crystallography. *Acta Crystallogr D* 1994;60:760–763.
7. Terwilliger TC, Kim SH. Generalized method of determining heavy-atom positions using the difference Patterson function. *Acta Crystallogr A* 1987;43:1–5.
8. Terwilliger TC, Berendzen J. Automated MAD and MIR structure solution. *Acta Crystallogr D* 1999;55:849–861.
9. Cowtan KD, Zhang KYJ. Density modification for macromolecular phase improvement. *Prog Biophys Mol Biol* 1999;72:245–270.
10. QUANTA. San Diego, CA: Molecular Simulations Inc.; 2000.
11. Brünger AT, Adams PD, Clore GM, DeLano WL, Gros P, Grosse-Kunstleve RW, Jiang J, Kuszewski J, Nilges M, Pannu NS, Read RJ, Rice LM, Simonson T, Warren GL. Crystallography & NMR system: a new software suite for macromolecular structure determination. *Acta Crystallogr D* 1998;54:905–921.
12. Kleywegt GJ, Jones TA. Databases in protein crystallography. *Acta Crystallogr D* 1998;54:1119–1131.
13. Laskowski RA, MacArthur MW, Moss DS, Thornton JM. PROCHECK—a program to check the stereochemical quality of protein structures. *J Appl Crystallogr* 1993;26:283–291.
14. Vaguine AA, Richelle J, Wodak SJ. SFCHECK: a unified set of procedures for evaluating the quality of macromolecular structure-factor data and their agreement with the atomic model. *Acta Crystallogr D* 1999;55:191–205.
15. Brunzelle JS, Wu R, Kozlov SV, Collart FR, Jouchimuk A, Anderson WF. Crystal structure of *Bacillus subtilis* YdaF protein: a putative ribosomal N-acetyltransferase. *Proteins* 2004;57:850–863.
16. Bateman A, Coin L, Durbin R, Finn RD, Hollich V, Griffiths-Jones S, Khanna A, Marshall M, Moxon S, Sonnhammer ELL, Studholme DJ, Yeats C, Eddy SR. The Pfam protein families database. *Nucleic Acids Res* 2004;32:D136–D121.
17. Newwald AF, Landsman D. GCN5-related histone N-acetyltransferases belong to a diverse superfamily that includes the yeast SPT10 protein. *Trends Biochem Sci* 1997;22:164–155.
18. Angus Hill ML, Duda RN, Tafrov ST, Sternglanz R, Kamakrishnan V. Crystal structure of the histone acetyltransferase Hpa2: a tetrameric member of the Gcn5-related N-acetyltransferase superfamily. *J Mol Biol* 1999;294:1311–1325.
19. Wybenga-Groot LE, Draker K, Wright GD, Berghuis AM. Crystal structure of an aminoglycoside 6'-N-acetyltransferase defining the GCN5-related N-acetyltransferase superfamily fold. *Structure* 1999;7:497–507.
20. Holm L, Sander C. The FSSP database of structurally aligned protein fold families. *Nucleic Acids Res* 1994;22:3600–3609.
21. Altschul SF, Madden TL, Schaffer AA, Zhang J, Zhang Z, Miller W, Lipman DJ. Gapped BLAST and PSI-BLAST: a new generation of protein database search programs. *Nucleic Acids Res* 1997;25:3389–3402.
22. Berman HM, Westbrook J, Feng Z, Gilliland G, Dhar TN, Weissig H, Shindyalov IN, Bourne PE. The Protein Data Bank. *Nucleic Acids Res* 2000;28:235–242.
23. DeLano WL. The PyMOL molecular graphics system. San Carlos, CA: DeLano Scientific; 2002.